Copper–dioxygen complexes: Functional models for proteins

Kenneth D. Karlin,* Dong-Heon Lee, Honorio V. Obias and Kristi J. Humphreys

Department of Chemistry, Charles and 34th Streets, The Johns Hopkins University, Baltimore, Maryland 21218, U. S. A.

The complex $[(\text{TMPA})\text{Cu}^{I}(\text{RCN})]^{+}$ (**1**) (TMPA = tris[(2-pyridyl)methyl]amine) binds O_2 forming $[\{(\text{TMPA})\text{Cu}\}_2(O_2)]^{2+}$ (**2**), with *trans*-μ-1, 2 peroxo-coordination. Study of complexes with binucleating ligand analogues provide considerable insights and achievement of room-temperature solution stability. Binucleating ligands with tridentate bis[(2-pyridyl)ethyl]amine chelates give side-on μ-η^2:η^2-peroxo dicopper(II) complexes, likewise in a monooxygenase model system. (P)Fe-X-Cu(L) (P = porphyrinate or binucleating tethered porphyrin; X = O^{2-}, OH⁻) oxidized resting state models of the heme a_3 and Cu_B site of cytochrome c oxidase have been generated and characterized, and reduced $(\text{P})\text{Fe}^{II}/\text{Cu}^{I}$ compounds, for O_2 reactivity studies, have been synthesized. A heme/non-heme diiron complex has been generated as a possible model for NO reductase.

INTRODUCTION

Copper containing proteins perform a diverse array of functions, all involving oxidation-reduction (i.e. 'redox') activity, since the types of ligands (e.g., histidine, tyrosine and cysteine) typically found in protein matrices facilitate, in particular, redox shuttling between reduced copper(I), and copper(II) oxidation states. Small 'blue' copper proteins carry out electron transfer reactions, for example as electron carriers in photosynthetic organisms. Other copper proteins effect redox reactions which involve atom transfer, such as those involving the processing of molecular oxygen (Table 1) (1-6) or nitrogen oxides (7).

TABLE 1. Main Classes of Copper Proteins involved in O_2-Processing (* X-ray Structures available).

PROTEIN	SOURCE	BIOLOGICAL FUNCTION
Oxygen Carrier		
Hemocyanin (Hc)*	Molluscs and Arthropods	O_2-transport
Copper Monoxygenases		
Tyrosinase (Tyr)	Fungal, Mammal	Tyrosine oxygenation
Dopamine β-hydroxylase (DβH)	Adrenal, Brain	Dopamine → Norepinephrine
Peptidylglycine α-Amidating Monooxygenase (PAM)	Pituitary, Heart	Oxidative N-dealkylation, Neuropeptide hormone biosyn.
Methane Monooxygenase (MMO)	Methanogenic bacteria	Methane → Methanol
Ammonia Monooxygenase	Bacteria	NH_3 → NH_2OH
Copper Dioxygenases		
Quercetinase	Fungal	Quercetin oxidative cleavage
Copper Oxidases		
Ascorbate Oxidase (AO)*	Plants	Oxidation of *l*-ascorbate
Laccase	Tree, Fungal	Phenol and diamine oxidation
Ceruloplasmin*	Human, Animal serum	Ferrioxidase activity ?
Amine oxidase*	Most animals	Elastin, Collagen formation
Galactose oxidase*	Molds	Galactose oxidation
Cytochrome c Oxidase (CcO)*	Mitochondria	Terminal oxidase (Proton pump)
Other		
Superoxide Dismutase (SOD)*	Red blood cells, Animals	O_2^- detoxification

Hemocyanins are blood O_2-transporting proteins (3,4). The deoxy state possesses three-coordinate cuprous ions (Cu...Cu = 4.6 Å) which bind O_2 to give a peroxo-dicopper(II) oxy form, with Cu...Cu = 3.6 Å, λ_{max} = 345 ($\varepsilon \sim 20,000$) and ν(O-O) $\sim$ 750 cm⁻¹ (resonance Raman). Monooxygenases (4,5) effect reactions involving oxygen-atom insertion *into* C-H bonds. Oxidases oxidize or dehydrogenate organic substrates, accompanied by O_2-reduction to either hydrogen peroxide or water (4). Cytochrome c

oxidases are mitochondrial terminal oxidases involved in O_2-reduction to water concomitant with energy transduction via proton pumping (8). Copper/zinc superoxide dismutase (SOD) is well characterized, and recent evidence suggests that a point mutation in the SOD gene may cause a degenerative disease of motor neurons, the inherited form of amyotrophic lateral sclerosis (ALS) (9).

deoxy-Hemocyanin   colorless   oxy-Hemocyanin   blue
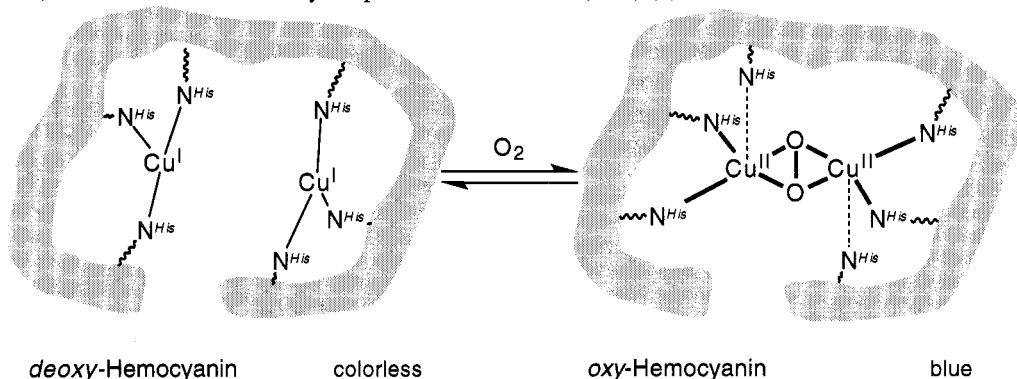
We, and others have endeavored to understand the structure and function of copper proteins involved in copper(I)/O_2 interactions, by studying inorganic models, i.e., synthetically derived copper(I) complexes, and their O_2-reactivity (2,3,6,10). Such biomimetic approaches can lead to fundamental insights into the metal-based chemistry, yielding an improved understanding of biological O_2-activation mechanisms, and the dependence of reactivity patterns upon the specific nature of Cu_n-O_2 structure. One might also envision the development of reagents or catalysts for use in practical oxidation processes. Here, we will highlight recent findings concerning the reversible binding of dioxygen to certain copper(I) complexes and O_2-activation chemistry We also wish to describe chemistry related to the dinuclear iron-copper center in cytochrome c oxidase (CcO).

## O_2-CHEMISTRY OF CU(I) COMPLEXES CONTAINING TRIPODAL LIGANDS

In order to model the neutral, aromatic, nitrogenous imidazolyl character observed in the histidyl-copper coordination found in hemocyanin and many other copper proteins, some of our studies have utilized synthetically accessible tripodal, tetradentate chelating pyridyl ligands, such as TMPA (TMPA = tris[(2-pyridyl)methyl]amine). The first X-ray structurally characterized Cu_2O_2 species, the trans-μ-1,2-peroxo [{(TMPA)Cu}$_2$(O_2)]$^{2+}$ (2), was formed from the reaction of [(TMPA)Cu(RCN)]$^+$ (1) with O_2 at -80 °C in EtCN or CH_2Cl_2 (Cu:O_2 = 2:1, manometry). The Cu(II) ions in 2 are pentacoordinate, the Cu-Cu distance is 4.359 Å and the O-O bond length is 1.432 Å (11a). [{(TMPA)Cu}$_2$(O_2)]$^{2+}$ (2) is intensely purple, displaying multiple strong O_2^{2-} to Cu(II) charge-transfer absorptions at λ_{max} = 440 nm (ε = 2000 $M^{-1}cm^{-1}$), 525 nm (11500), and 590 nm (sh, 7600). In addition, there is a d-d band at 1035 nm (180). Although O_2 binds strongly to complex 1 at low temperatures, it can be removed reversibly by vacuum cycling experiments, i.e., application of vacuum while the solution is subjected to brief heating. Resonance Raman studies of 2 show an O-O stretch (832 cm^{-1}) and a Cu-O stretch (561 cm^{-1}) (11b). Complex 2 also exhibits silent EPR and nearly normal ^1H NMR spectra. Magnetic susceptibility measurements performed on 2 indicate that -2J > 600 cm^{-1}, based on $H = 2JS_1 \cdot S_2$. These results show that a single bridging O_2^{2-} ligand can mediate strong magnetic coupling between two Cu(II) ions. Although 2 is a functional model for hemocyanin, it lacks the precise spectroscopic and structural signatures of the active site of oxy-hemocyanin (vide supra), wherein η^2:η^2 O_2^{2-} to dicopper(II) binding has been determined (3,4). Kitajima and coworkers (3) have achieved the synthesis and structural/spectroscopic characterization of a model compound duplicating those properties observed in oxy-hemocyanin, using sterically hindered tridentate tris(pyrazolyl)borate ligands.

TMPA   1   2
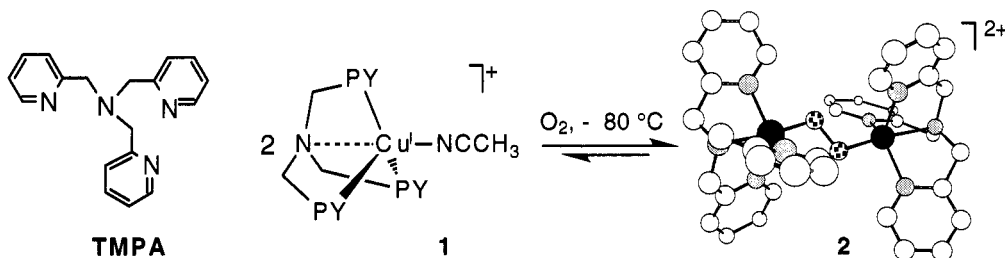
Kinetic/Thermodynamics Investigations and Comparisons with Dinucleating Analogues.

Kinetic/thermodynamic investigations carried out in collaboration with Professor A. D. Zuberbühler and co-workers in Basel, Switzerland, have revealed the formation of a primary 1:1 Cu/O_2 adduct in the reaction of O_2 with [(TMPA)Cu(RCN)]$^+$ (**1**) and in a quinolyl analogue (**6**). [(TMPA)Cu(O_2)]$^+$ (**1'**) forms as a spectroscopically observable (λ_{max} = 410 nm) transient (k_1 = 1.8 x 10^4 M^{-1}s^{-1}, K_1 = 1.9 x 10^3 at -90 °C; $\Delta H°$ = -34 kJ/mol, $\Delta S°$ = -123 J/K-mol); extrapolation to room temperature gives an O_2 on-rate of ~ 10^8 M^{-1}s^{-1} (**6**). This compares with or exceeds the O_2-binding rate for heme proteins or iron-porphyrin complexes, many cobalt(II) chelates, and is comparable to the oxygenation rate of *deoxy*-hemocyanin.

More recently, we have synthesized dinucleating analogues, D^1 and DO, providing new insights and the ability to stabilize Cu_2O_2 adducts at room temperature in solution, a long elusive goal in the field. In EtCN solvent, the dicopper(I) complex [(D^1)Cu$^I_2$-(EtCN)$_2$]$^{2+}$ (**3**) proceeds to give an intramolecular peroxodicopper(II) product [(D^1)Cu$^{II}_2$(O_2^{2-})]$^{2+}$ (**5**, L = D^1, λ_{max} = 540 nm), analogous to [{(TMPA)Cu}$_2$-(O_2)]$^{2+}$ (**2**). However, a detailed analysis reveals that while D^1 helps to overcome the entropic handicap inherent in formation of **2**, the -CH$_2$CH$_2$- linker in D^1 causes steric constraints making product **5** strained (**6**). Activation enthalpies for formation of **5** are 20 kJ mol^{-1} higher for dioxygen binding (k_2, k_{on} = k_1k_2/k_{-1}), but more than 20 kJ mol^{-1} lower for Cu-O bond splitting (k_{-2}), as compared to **2**. The net result is a massive loss in overall enthalpy of formation, $\Delta H_{on}°$, reduced to -35 kJ mol^{-1} for **5** (L = D^1) compared to -81 kJ mol^{-1} for **2**. Ring closure (i.e., peroxo formation) itself (K_2) has a slightly endothermic reaction enthalpy, 0.5 kJ mol^{-1} (**6**). The strain in fact results in a rearrangement at higher temperatures (> ~ -50 °C), leading to the formation of a trimer, [{(D^1)Cu$^{II}_2$(O_2^{2-})}$_3$]$^{6+}$, with *inter*molecular μ-peroxo moieties.
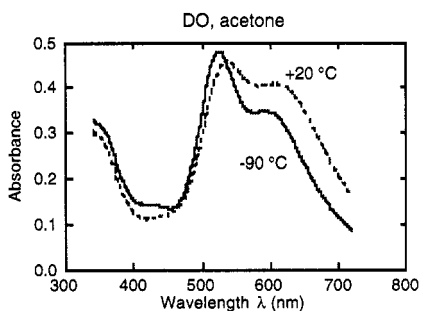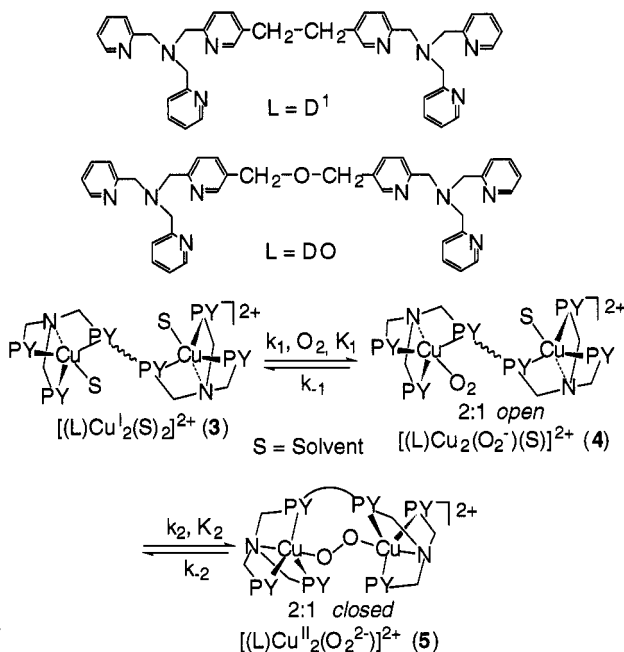

We find that acetone as a solvent (compared to EtCN) confers considerable room temperature stability to **5** (L = D^1), K_1K_2 > 4 x 10^3 M^{-1} and $t_{1/2}$ (decomp.) ~ 40 s. With DO as the dinucleating ligand, the longer more flexible -CH$_2$OCH$_2$- linker apparently overcomes the steric constraints observed for the D^1 complex. Surprisingly, we do not observe formation of Cu/O_2 1:1 adducts such as **4** for L = DO; [(DO)Cu$^{II}_2$(O_2^{2-})]$^{2+}$ (**5**) is formed rapidly and with great stability, even at room temperature. [(DO)Cu$^{II}_2$(O_2^{2-})]$^{2+}$ (**5**, L = DO) fully forms at room temperature (as shown by the accompanying spectra at -90 °C compared to +20 °C) with $t_{1/2}$ (decomp.) ~ 60 s (**12**).


O_2-BINDING/ACTIVATION WITH TRIDENTATE LIGAND COMPLEXES

Another class of compounds we have studied use dinucleating ligands where two bis[2-(2-pyridyl)ethyl]amine (PY2) units are linked through the amino nitrogens by a variable -(CH$_2$)$_n$- (n = 3-5) hydrocarbon spacer (3,10,13). For tricoordinate complexes [Cu$_2$(Nn)]$^{2+}$ (**6**) or tetracoordinate nitrile adducts [Cu$_2$(Nn)(CH$_3$CN)$_2$]$^{2+}$ (**6a**), reversible binding has been demonstrated. These react with O_2 at -80 °C in CH$_2$Cl$_2$ solution, producing deep brown or purple species [Cu$_2$(Nn)(O_2)]$^{2+}$ (**8**). As found for our other copper dioxygen complexes, reversible O_2 and CO binding can be followed

spectrophotometrically. Carbon monoxide binding to **6** is stronger than O_2, since CO can displace O_2 from **8** to give $[Cu_2(Nn)(CO)_2]^{2+}$ (**7**). The relative binding strength of CO vs. O_2 to reduced copper ion parallels that observed for heme-proteins and porphyrin-iron(II) complexes.
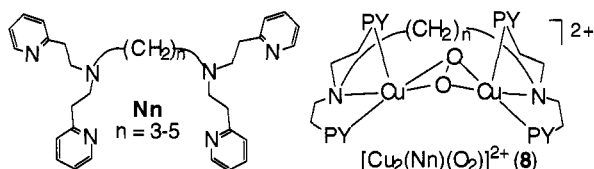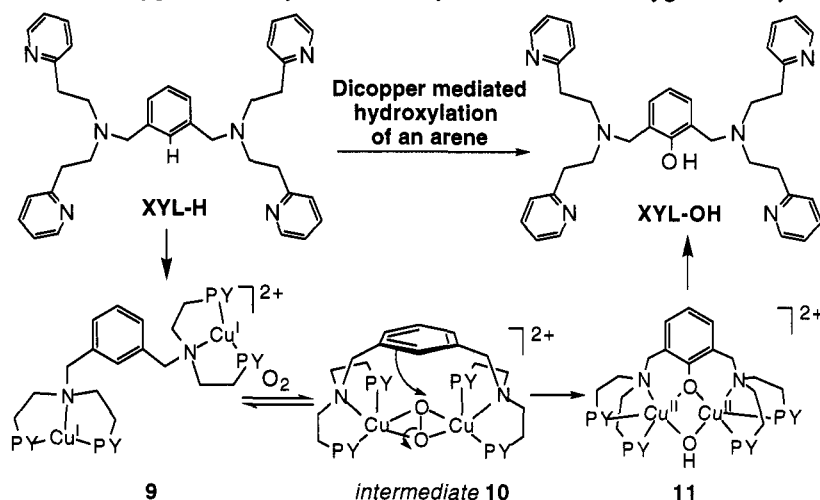
Complexes $[Cu_2(Nn)(O_2)]^{2+}$ (**8**) possess striking UV-VIS properties, in particular a characteristic 350-360 nm band with ε=16-21000 $M^{-1}cm^{-1}$. The strong 350-360 nm band is characteristic of μ-η^2:η^2 side-on peroxo coordination as seen with Kitajima's complex and oxy-hemocyanin (3); recent resonance Raman measurements on complexes **8** confirm this supposition. The position and relative intensity of a variable 400-500 nm absorption varies systematically with n, reflecting subtle changes in the mode of O_2 binding or the geometry of the Cu_2-(O_2) moiety. X-ray absorption measurements carried out on the N3 and N4 derivatives confirm the Cu(II) oxidation state (XANES, near-edge structure), while also allowing determination of Cu$\cdots$Cu distances, which are 3.3 and 3.4 Å, respectively. Thus, the data are consistent with a bent 'butterfly' μ-η^2:η^2-peroxo dicopper(II) structure for $[Cu_2(Nn)(O_2)]^{2+}$ (**8**), as shown; the distortions from planarity are seen to arise from constraints associated with the binucleating Nn ligand. As with oxy-hemocyanin, $[Cu_2(Nn)(O_2)]^{2+}$ (**8**) complexes are EPR silent and diamagnetic (3,10,13).
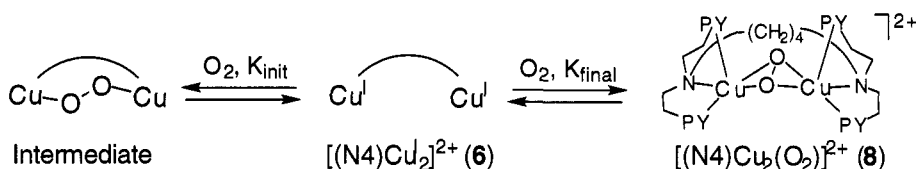
A recent insight into the dynamics associated with copper-dioxygen complex formation comes from a kinetic study of the formation of $[Cu_2(N4)(O_2)]^{2+}$ (**8**) from oxygenation of the dicopper(I) complex, $[Cu_2(N4)]^{2+}$ (**6**) (6,14). A considerable binding strength is associated with μ-η^2:η^2-peroxo formation in $[Cu_2(N4)(O_2)]^{2+}$ (ΔH° = -58 kJmol^{-1}), which is compensated by a reaction entropy of ΔS° = -165 JK^{-1}mol^{-1}. Most interestingly, at low temperatures, formation of this product is preceded by a less stable intermediate (ΔH° = -28 kJmol^{-1}) whose spectral characteristics (λ_{max} = 525 nm) implicate 'end-on' peroxo ligation. End-on to side-on peroxo conversion is likely to induce significant shortening of the Cu...Cu distance from ~ 4.4 Å to 3.3-3.7 Å. Since Cu...Cu = 4.6 Å in deoxy-hemocyanin, but 3.6 Å in oxy-hemocyanin, we suggest that an analogous thermodynamically driven rearrangement may be the basis for initiating subunit-subunit cooperativity in hemocyanin O_2-binding (6,14).

A Monooxygenase Model System

When the linker between PY2 moieties is a *m*-xylyl group (XYL-H), formation of a dicopper(I) complex **9** leads to dioxygen reactivity which closely resembles monooxygenase enzymes s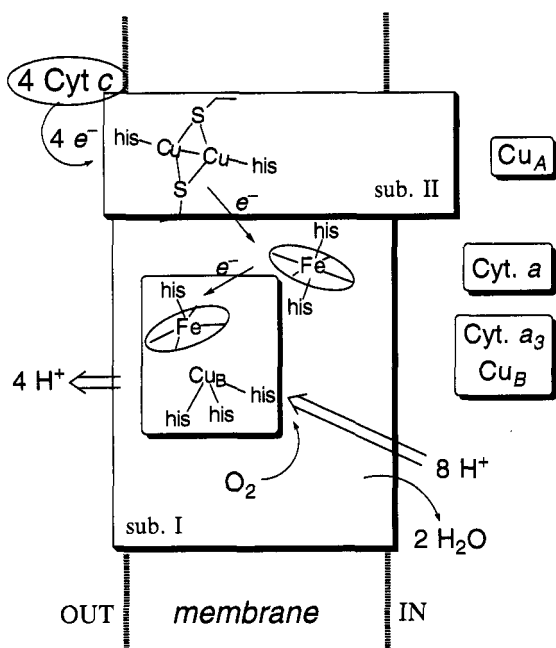uch as tyrosinase, with C-H activation incorporating one O atom from O_2 into the ligand substrate. The product is the phenoxo and hydroxo-bridged dicopper(II) complex **11**, from which the hydroxylated ligand XYL-OH can be extracted, completing the dicopper mediated hydroxylation of an arene, under very mild conditions (1 atm O_2). Isotopic labeling experiments and the observed stoichiometry of reaction (Cu/O_2 = 2:1) are that expected of a monooxygenase. Detailed mechanistic studies reveal that a Cu_2-O_2 intermediate **10** forms (reversibly) upon reaction of **9** with O_2. The side-on μ-η^2:η^2-peroxo structure (shown) for **10** is inferred by spectroscopic analogy to $[Cu_2(N4)(O_2)]^{2+}$ (**8**) and from recent resonance Raman studies on a derivative in which the intermediate

10 is stabilized at low temperatures by the presence of an electron withdrawing -NO_2 group para to the xylyl ring position which becomes hydroxylated. Thus, as in the enzyme active site, the peroxo group in **10** is located in highly favorable proximity to the xylyl ligand substrate, and facile hydroxylation occurs by electrophilic attack on the arene substrate π system. An "NIH shift" mechanism is involved, like that previously established for iron hydroxylases (6,10,15).

MODELS FOR THE Fe-Cu DINUCLEAR SITE IN CYTOCHROME *c* OXIDASE

Cytochrome *c* oxidase (C*c*O) is a terminal respiratory protein which catalyzes the four-electron four-proton reduction of O_2 to water. The process is coupled to proton translocation across the cell membrane. The electrochemical potential gradient generated by this proton pumping process is ultimately used in the synthesis of ATP (8). Electrons are transferred to a binuclear cysteine-bridged mixed-valent dicopper (Cu_A) center in subunit II. A low-spin heme a_3 is also involved in electron transfer, but the critical O_2-reduction site is the binuclear metal site consisting of a high-spin heme a_3 and closely neighboring Cu_B-$(N_{histidine})_3$ moiety. Recent enzyme x-ray crystal structures are available (8).

Considerable biochemical and inorganic modeling research efforts have focused on aspects of the 'as-isolated' resting oxidized state of the dinuclear center, which may possess a spin-coupled ($-J > 50$ cm^{-1}) Fe^{III}-X-Cu^{II} center. With our experience with copper(I)/O_2 chemistry, we have also been very interested in functional modeling (2,10) of C*c*O, i.e. O_2-reaction chemistry involving reduced metals, with copper(I) and porphyrin-iron(II) species. For the enzyme, kinetic and spectroscopic evidence point to Cu_B as the initial binding site for O_2, thus highlighting the importance of Cu(I)-O_2 reactivity in the O_2 reduction process of C*c*O (8). It is known that the O_2-ligand transfers to the heme a_3 forming an adduct analogous to that seen in hemoglobin.

Following this and injection of further reducing equivalents, the bound O_2 is rapidly converted to other intermediates including an O-O cleaved spectroscopically detectable ferryl Fe^{IV}-oxo species. The resting oxidized state is regenerated after the fourth electron transfer and protonation to give water (8).

Synthesis and Characterization of Oxo/Hydroxo Bridged Iron-Copper Dinuclear Complexes

In our initial attempts to delve into this type of chemistry, we chose to use TMPA-Cu complexes, since the O_2-reactivity of $[(TMPA)Cu^I$ -$(CH_3CN)]^+$ (**1**) is most understood. When an equimolar mixture of (F_8-TPP)Fe^{II} (or an analogue with axial piperidine ligands) and **1** is reacted in the presence of dioxygen, $[(F_8$-TPP)Fe^{III}-(O^{2-})-Cu^{II}-(TMPA)]^+ (**12**) is isolated. The same complex, identified by its UV-Vis and NMR spectroscopic properties, can also be generated via an acid-base self-assembly reaction, by mixing equimolar amounts of $[(TMPA)Cu^{II}(CH_3CN)]^{2+}$, ($F_8$-TPP)$Fe^{III}$-OH, and Et_3N in CH_3CN solvent.
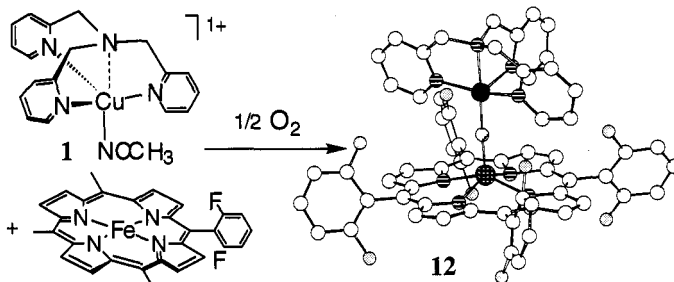
The structure of $[(F_8$-TPP)Fe^{III}-(O^{2-})-Cu^{II}(TMPA)]^+ (**12**) reveals a linear Fe(III)-oxo-Cu(II) coordination ($\angle$ Fe-O-Cu = 178.2°), with short Fe-O (1.740 Å, similar to μ-oxo bridged iron-porphyrin dimers) and Cu-O (1.856 Å) bond lengths. Physical measurements indicate **12** is an S = 2 spin system, with high-spin iron(III) strongly antiferromagnetically coupled (J = -87 cm^{-1} (solid), where $H = -2J S_1 \cdot S_2$) to an S = 1/2 Cu(II) ion center (16). This magnetic behavior gives rise to unusual ^{1}H-NMR spectroscopic properties,

with resonances at room temperature ranging from +65 ppm downfield to -104 ppm (upfield). The spectrum has been fully assigned and the NMR and electronic properties of **12** and its protonated analogue (vide infra) discussed in terms of current theory (17).
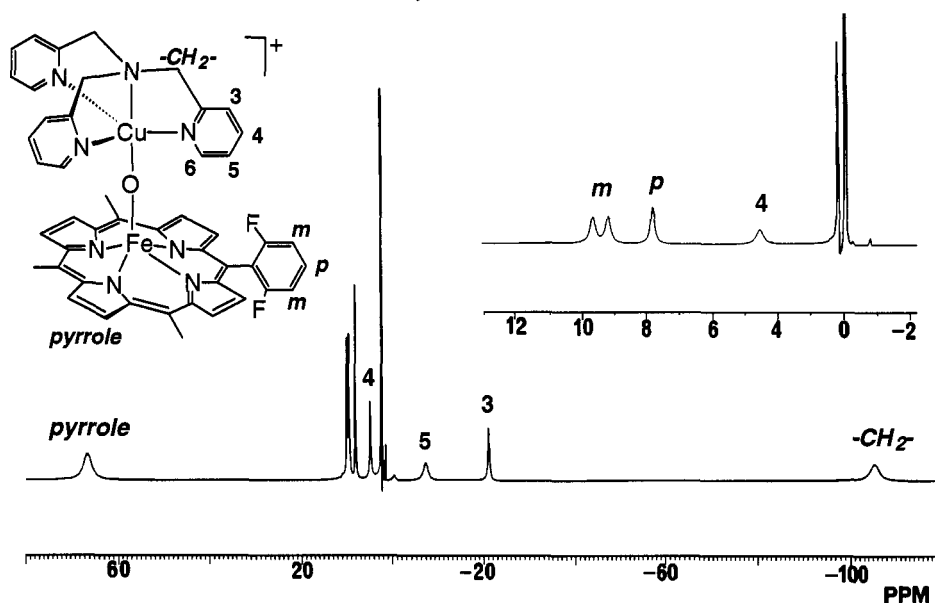

Protonation of $[(F_8\text{-TPP})Fe^{III}\text{-}(O^{2-})\text{-}Cu^{II}(TMPA)]^+$ (**12**) by addition of one equivalent of H^+ produces the hydroxo-bridged complex, $[(F_8\text{-TPP})Fe\text{-}(OH)\text{-}Cu(TMPA)]^{2+}$ (**13**). This can also be isolated by reacting an equimolar mixture of $[(TMPA)Cu^{II}(CH_3CN)]^{2+}$ and $[(F_8\text{-TPP})Fe\text{-}OH]$. Extended X-ray Absorption Fine Structure spectroscopy (EXAFS) measurements indicate **13** possesses elongated Fe-OH and Cu-OH

bonds and a bending such that $\angle$ Fe-O-Cu $\cong$ 157°(18). This results in a loss of the outer shell strong multiple scattering observed in **12**, due to its linear Fe-O-Cu moiety. We have suggested (18) that **13** is a plausible model for the resting ('as-isolated) oxidized enzyme, with its supposed Fe-X-Cu antiferromagnetic coupling. Since protonation of enzyme turnover intermediates leads to product water and/or translocated protons, it is of interest that the oxo moiety in **12** is basic; we estimate that $14 < pK_a < 17$ in CH_3CN ($pK_a \sim 8 \pm 2.5$ in water) (18).
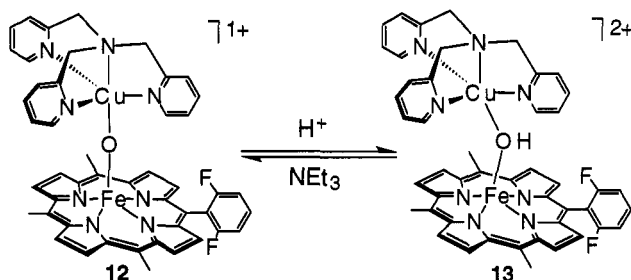
Isotopic labeling of the dioxygen reacted with $(F_8\text{-TPP})Fe^{II}$ and **1** to give **12** indicates that the oxo group in the product is derived from O_2, as judged by a new isotope sensitive IR band at 856 cm^{-1}. Manometry reveals an $Fe/Cu/O_2$ = 2:2:1 stoichiometry. Thus, our reaction system represents a crude functional model for C*c*O. While the mechanism of reaction of this Fe/Cu O-O bond cleavage reaction is of interest, we have instead chosen to turn our focus of structural, reactivity and mechanistic studies to the use of analogous systems involving binucleating ligands, such as ⁵L and ⁶L, where Ar = 2,6-difluorophenyl (19).
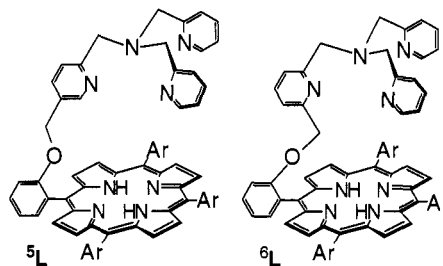
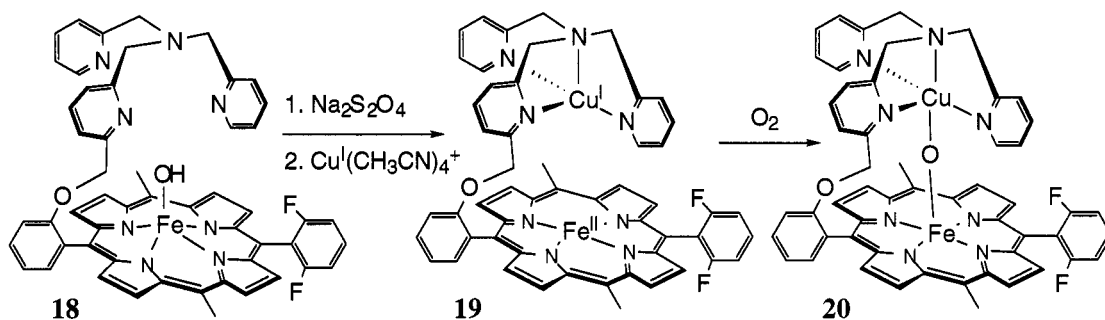## Chemistry of Binucleating Ligands with TMPA Tethered to Porphyrins

Introduction of ferric chloride to the binucleating ligand, ⁵L, leads to the isolation of $[(^5L)Fe\text{-}O\text{-}Fe(Cl)]^+$ (**14**), containing both heme and non-heme iron(III) bridged by an oxide atom (20). Complex **14** is characterized by UV-Vis bands at 411 (Soret) and 564 nm. Mössbauer spectroscopy reveals distinctive

Fe(III) sites, both being high-spin. ^{1}H-NMR resonances in the 0-30 ppm range and magnetic properties (3.4 μ_B/Fe at room-temperature) are consistent with the presence of antiferromagnetic coupling through the oxo-bridge in **14**. An IR band at 835 cm^{-1} is assigned to an Fe-O-Fe asymmetric stretch; this shifts to 801 cm^{-1} upon treatment of the compound with $H_2^{18}O$. The X-ray structure reveals short Fe-O bonds; Fe...Fe' = 3.484 Å, $\angle$ Fe-O-Fe = 157.3°. The bending is not seen as being caused by ligand constraints since a close analogue without tethered porphyrin binucleating ligand and which can be generated by acid-base self-assembly, [(F$_8$-TPP)Fe-O-Fe(TMPA)(Cl)]$^{2+}$ (**14'**) possesses a very similar structure (20).

Heme/non-heme complexes **14** and **14'** may have biological relevance, since denitrifying bacterial nitric oxide reductases are evolutionarily related to heme-copper oxidases and possess a heme center with additional non-heme iron atom (21). Thus, this postulated binuclear center may comprise the catalytic core responsible for the reductive coupling of 2NO giving N_2O and an oxo species like **14**. Preliminary experiments suggest we may be able mimic this kind of behavior. Treatment of **14** with dithionite gives a reduced di-iron(II) species (in situ), which upon exposure to $NO_{(g)}$ gives back **14**. Detection of N_2O is also suggestive; further experimentation and characterization is needed.
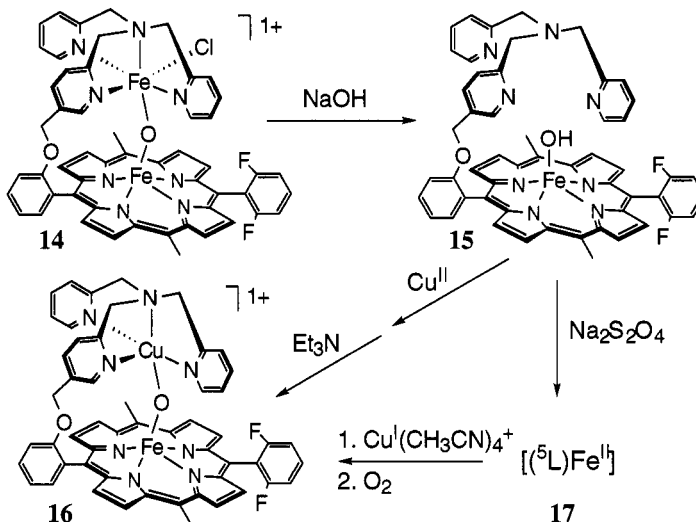
The ligand ^{5}L also allows generation of complexes of interest for modeling *Cc*O. 'Rusting' out of the non-heme iron ion from **14** gives a high-spin Fe^{III}-OH complex, [(^{5}L)Fe-OH] (**15**), with an empty tether. Addition of a copper(II) salt and base gives [(^{5}L)Fe-O-Cu]$^+$ (**16**) as judged by its UV-Vis and ^{1}H-NMR properties, which parallel those of [(F$_8$-TPP)Fe^{III}-(O^{2-})-Cu^{II}(TMPA)]$^+$ (**12**). Reduction of **15** gives an iron(II) species, **17**, to which addition of copper(I) and O_2 also gives **16**. The characterization and reactivity studies of a reduced Fe-Cu complex such as [(^{5}L)Fe...Cu]$^+$ are currently being pursued.

Similar chemistry can be achieved with the ^{6}L binucleating ligand. An iron(III) complex with an empty TMPA tether analogous to **15** can be isolated, i.e., [(^{6}L)Fe-OH] (**18**). Reduction of this with dithionite and addition of a copper(I) salt afford **19**; this is a reduced iron (II)-copper(I) complex, with λ_{max} = 424 nm, and with NMR properties consistent with high-spin Fe(II) (tetrahydrofuran (THF) solvent). Reaction with O_2 affords the Fe(III)-O-Cu(II) complex, [(^{6}L)Fe-O-Cu]$^+$ (**20**), as judged by UV-Vis, ^{1}H NMR and X-ray structural properties. EXAFS and X-ray structural studies also reveal significant structural differences in the Fe-oxo-Cu complexes **16** and **20**, undoubtedly caused by the differences in ligand contraints imposed by the ligands ^{5}L versus ^{6}L. Another exciting preliminary observation is that when we carry out the oxygenation of **19** at -80 °C in THF solvent. a new spectroscopically distinct species is observed. This bodes well for future investigations where we wish to probe the possibility of forming Fe-peroxo-Cu or other interesting intermediates which may have relevance to the processes of O_2-binding, reduction, O-O cleavage and proton translocation by the Fe-Cu center in cytochrome *c* oxidases.

SUMMARY/CONCLUSION

Copper proteins involved in dioxygen binding or activation possess a variety of active site structures and chemistry. Such observations have led us to utilize a variety of ligands to develop model compounds and reaction chemistry which can provide information about fundamental aspects of copper complex interactions and reactions with O_2. [(TMPA)Cu^I(RCN)]$^+$ (**1**) binds O_2 reversibly at -80 °C to give the Cu/O_2 = 2:1 ($Cu:O_2$) *trans*-μ-1, 2-peroxo adduct [{(TMPA)Cu}$_2$(O_2)]$^{2+}$ (**2**). This structure is not that found in the biological O_2-carrier protein hemocyanin, but this and other studies indicate that biomimetic reversible O_2-binding in synthetic copper complexes can be studied, and that a number of Cu_n-O_2 binding modes are possible. The binucleating analogues, D^1 and DO, provide insights about the relative stabilities of peroxo-dicopper(II) complexes, intra vs. inter-molecular copper-dioxygen binding, and how ligand design can lead to Cu_2-O_2 complexes which are stable at room temperature in solution. Binucleating ligands with two connected bis[2-(2-pyridyl)ethyl]amine (PY2) units lead to dicopper(I) complexes which also reversibly bind O_2 (and CO), and which have the μ-η^2:η^2 side-on peroxo coordination seen in oxy-hemocyanin. Small changes in the ligand, i.e. the nature of the linker between PY2 moieties, causes spectroscopic and structural changes in the Cu_2-O_2 moiety. When the linker is a *m*-xylyl moiety, a model system for copper monooxygenation has been characterized, since oxygenation of the dicopper(I) in that system (XYL ligand) results in the facile and regiospecific hydroxylation of the xylyl ring. Mechanistic studies implicate a μ-η^2:η^2-peroxo intermediate which attacks the substrate in an electrophilic reaction. Our attention in the last few years has also turned to studies aimed at modeling the Fe-Cu binuclear center of cytochrome *c* oxidases. An initial biomimetic reaction utilizes **1**, (F_8-TPP)Fe^{II} and O_2, which produces the oxo-bridged complex, [(F_8-TPP)Fe^{III}-(O^{2-})-Cu^{II}(TMPA)]$^+$ (**12**). Recent efforts with the binucleating ligands, ^5L and ^6L, having a TMPA moiety tethered to a porphyrin periphery are leading to exciting new chemistry, including the heme/non-heme diiron complex, [(^5L)Fe-O-Fe(Cl)]$^+$ (**14**), as a model for NO reductase, Fe-Cu complexes analogous to **12**, and the ability to produce reduced Fe(II)-Fe(II) and Fe(II)-Cu(I) complexes for future reactivity investigations.

REFERENCES

(1)   K.D. Karlin and Z. Tyeklár, Eds., *Bioinorganic Chemistry of Copper*, Chapman & Hall, NY (1993).
(2)   K.D. Karlin, *Science*, **261**, 701-708 (1993).
(3)   N. Kitajima and Y. Moro-oka, *Chem. Rev.* **94**, 737 (1994).
(4)   E.I. Solomon, U. M. Sundaram and T. E. Machonkin, *Chem. Rev.*, **96**, 2563-2605 (1996).
(5)   J. P. Klinman, *Chem. Rev.*, **96**, 2541-2561 (1996).
(6)   K.D. Karlin, S. Kaderli and A.D. Zuberbühler, *Acc. Chem. Res.*, **30**, 139-147 (1997).
(7)   B.A. Averill, *Chem. Rev.*, **96**, 2951-2964 (1996). W.G. Zumft and P.M.H. Kroneck, *Adv. Inorg. Biochem.*, **11**, 193-221 (1996).
(8)   S. Ferguson-Miller and G. T. Babcock, *Chem. Rev.*, **96**, 2889-2907 (1996) and refs. cited therein.
(9)   I. Fridovich, *Annu. Rev. Biochem.*, **64**, 97-112 (1995).
(10) (a) K.D. Karlin, Z. Tyeklár, and A.D. Zuberbühler, *Bioinorganic Catalysis*, **261**, Marcel Dekker, NY (1992). (b) K. D. Karlin and Z. Tyeklár, *Adv. Inorg. Biochem.*, **9**, 123-172 (1994).
(11) (a) Z. Tyeklár, R. R. Jacobson, N. Wei, N. Narasimha Murthy, J. Zubieta and K. D. Karlin, *J. Am. Chem. Soc.* **115**, 2677-2689 (1993). (b) M.J. Baldwin, P.K. Ross, J.E. Pate, Z. Tyeklár, K.D. Karlin, and E.I. Solomon, *J. Am. Chem. Soc.* **113**, 8671-8679 (1991).
(12) K.D. Karlin, D.-H. Lee, S. Kaderli and A. D. Zuberbühler, *Chem. Commun.*, 475-476 (1997).
(13) K. D. Karlin, Z. Tyeklár, A. Farooq, M. S. Haka, P. Ghosh, R. W. Cruse, Y. Gultneh, J. C. Hayes, P. J. Toscano and J. Zubieta, *Inorg. Chem.*, **31**, 1436-1451 (1992).
(14) B. Jung, K.D. Karlin and A. D. Zuberbühler, *J. Am. Chem. Soc.* **118**, 3763-3764 (1996).
(15) K. D. Karlin, M. S. Nasir, B. I. Cohen, R. W. Cruse, S. Kaderli and A. D. Zuberbühler, *J. Am. Chem. Soc.*, **116**, 1324-1336 (1994).
(16) K.D. Karlin, A. Nanthakumar, S. Fox, N.N. Murthy, N. Ravi, B.H Huynh, R.D. Orosz and E.P. Day, *J. Am. Chem. Soc.* **116**, 4753-4763 (1994).
(17) A. Nanthakumar, S. Fox, N.N. Murthy and K. D. Karlin, *J. Am. Chem. Soc.* **119**, 3898-3906 (1997).
(18) S. Fox, A. Nanthakumar, M. Wikström, K. D. Karlin and N. J. Blackburn, *J. Am. Chem. Soc.* **118**, 24-34 (1996).
(19) K. D. Karlin, S. Fox, A. Nanthakumar, N. N. Murthy, N. Wei, H. V. Obias, and C. F. Martens, *Pure & Appl. Chem.*, **67**, 289-296 (1995).
(20) C. F. Martens, N. N. Murthy, H. V. Obias and K. D. Karlin, *Chem. Commun.*, 629-630 (1996).
(21) P. Girsch and S. de Vries, *Biochim. Biophys. Acta*, **1318**, 202-216 (1997).